Mass-Sensitive Detection of Gas-Phase Volatile Organics Using Disk Microresonators

ARTICLE *in* ANALYTICAL CHEMISTRY · APRIL 2011

Impact Factor: 5.64 · DOI: 10.1021/ac1029902 · Source: PubMed

analytical chemistry

ARTICLE

pubs.acs.org/ac

Mass-Sensitive Detection of Gas-Phase Volatile Organics Using Disk Microresonators

Stuart B. Truax,*[,†] Kemal. S. Demirci,[‡] Luke A. Beardslee,[†] Yulia Luzinova,[⊥] Andreas Hierlemann,[§] Boris Mizaikoff,[∥] and Oliver Brand[†]

[†]Georgia Institute of Technology, School of Electrical and Computer Engineering, Atlanta, Georgia 30332, United States

[‡]Now at Texas Instruments, Dallas, Texas, United States 75243

[⊥]Now at Center for Disease Control, Atlanta, Georgia, United States 30333

[§]Bioengineering Laboratory, Department of Biosystems Science and Engineering, ETH Zurich, Basel, Switzerland

[∥]Institute of Analytical and Bio-analytical Chemistry, University of Ulm, Ulm, Germany

ABSTRACT: The detection of volatile organic compounds (VOCs) in the gas phase by mass-sensitive disk microresonators is reported. The disk resonators were fabricated using a CMOS-compatible silicon micromachining process and subsequently placed in an amplifying feedback loop to sustain oscillation. Sensing of benzene, toluene, and xylene was conducted after applying controlled coatings of an analyte-absorbing polymer. An analytical model of the resonator's chemical sensing performance was developed and verified by the experimental data. Limits of detection for the analytes tested were obtained, modeled, and compared to values obtained from other mass-sensitive resonant gas sensors.

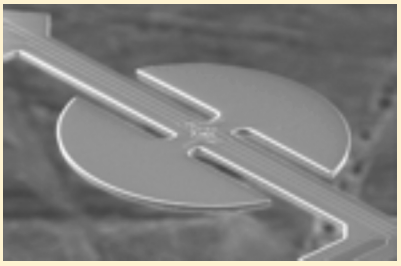

Gravimetric sensing of chemical analytes has been explored since King used quartz-crystal microbalances (QCMs) to detect volatile organic compounds (VOCs) in 1964.[1] Gravimetric approaches involve a mass change on the surface of a transducer. The addition of mass to a transducer surface can affect either (a) the static bending of the transducer through surface stress (static mode), or (b) the propagation of elastic waves through the transducer (dynamic mode). A pervasive and easily modeled sensor structure is the cantilever, which consists of a beam with one fixed end and one free end. Cantilever structures are extensively studied and can have mass sensitivities in the zeptogram range.[2] Cantilever structures can employ either static or dynamic modes of operation. Static-mode cantilevers coated with analyte-sensitive surfaces have been used to detect parts-per-trillion (ppt) concentrations of anlaytes such as TNT[3] and parts-per-billion (ppb) concentrations of methylphosphate vapor.[4] The static deflection of these cantilever sensors can be detected with integrated piezoresistors or with the aid of a laser. The static mode allows for robust operation in viscous media[5,6] but requires that significant calibration be performed to determine the concentration−deflection relationship particular to the sensor.

Dynamic-mode gravimetric sensors are typically employed as resonators whose oscillation is sustained by an amplifying feedback loop. The relative simplicity of this configuration has allowed resonator-based sensor systems to grow in prominence. The output of a sensor system employing dynamic-mode sensors is the oscillation frequency of the feedback loop. This oscillation frequency is modulated by the sorption and desorption of analyte on the sensing structure. Surface acoustic wave (SAW) and bulk acoustic wave (BAW) sensors are common resonator types which use piezoelectric materials to actuate the oscillation. SAW devices coated with absorbing polymers have been employed in the liquid phase to detect concentrations of VOCs in the 10s of ppb.[7,8] Gas phase detection of VOCs in the low ppb range by SAW sensors using preconcentrators has also been reported.[9−11]

The frequency stability of the resonator structure determines the noise floor of the sensor output signal. Frequency noise has several sources, including a significant contribution from statistical thermal noise. Noise in the frequency signal is related to the resonator Q-factor, through a $1/Q$ or $1/Q^2$ relationship[12,13] depending on the noise source. Therefore, resonators with a high Q-factor are preferred in mass-sensing applications.

Since mass-sensing resonators are often employed in viscous media such as gases or liquids, the energy loss from viscous damping can significantly reduce the Q-factor, in turn reducing the mass resolution of the sensor. The dynamic mode of the sensor can be altered to reduce this effect. An example is the use of in-plane modes as opposed to out-of-plane modes to eliminate normal stresses on the resonator surface from the surrounding fluid.[14,15]

The presence of viscous media also dictates the actuation scheme used to sustain oscillation. Electrostatic actuation uses the force generated by electric fields acting on charged electrodes to sustain oscillation. This scheme often requires submicrometer gaps between the driving electrodes, creating the possibility of energy loss due to squeeze-film damping. Electrostatic actuation

Received: November 18, 2010
Accepted: March 9, 2011
Published: April 06, 2011

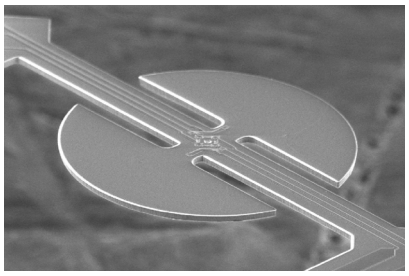

Figure 1. SEM micrograph of the disk resonator.

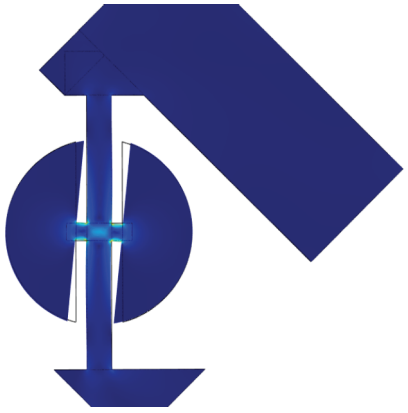

Figure 2. FEM simulation of the in-plane resonance mode (top view). Coloring shows von Mises stress distribution.

of silicon cantilever structures with integrated CMOS readout circuity has been demonstrated in chemical sensor applications in the gas phase,[16] but application of these structures in the liquid phase is challenging.

Electrothermal actuation uses a temperature gradient to create a mechanical deflection. This technique is advantageous in that the required heat source can be implemented by an integrated resistor which is part of the bulk sensor structure. This transduction mechanism has been demonstrated to actuate resonators with resonance frequencies in the GHz range[17] and is easily implemented in silicon using standard CMOS doping processes. Silicon cantilever resonators with integrated readout circuitry using electrothermal excitation have been demonstrated in the detection of VOCs in the gas phase.[18,19] However, the use of resonators operating in an in-plane resonance mode using electrothermal excitation for gas-phase detection of VOCs is newly reported in this research.

SYSTEM DESIGN

The chemical sensor system studied in this research uses a silicon-based resonator vibrating in an in-plane resonance mode. The silicon disk-type structure is suspended by two anchor beams measuring 250 μm lengthwise. The disks used in this research have a radius of 170 μm with a 20 μm gap between the half-disks and the central anchor beam. The in-plane resonance mode constitutes a small-angle rotation of the half-disks about the central anchor point. Figure 1 shows an SEM micrograph of the disk resonator. Figure 2 shows a finite element (FEM) simulation of the disk resonator's in-plane resonance mode.

Viscous damping of this resonator structure has been reduced through the use of an in-plane resonance mode. Cantilever structures typically use out-of-plane resonance modes, and silicon-based cantilevers of this type have Q-factors at most on the order of 1500[20] in air. The Q-factor limit of cantilevers is a result of energy loss to normal stresses from the surrounding fluid media (e.g., the atmosphere) and loss due to energy storage in the associated support structures (i.e., support loss). In-plane modes help to eliminate these normal stresses. The disks used in this research have previously been shown to achieve Q-factors of 5800 for a 5 μm thick device in air.[15]

The gap distance between the half-disks and the central anchor beam was chosen to be 20 μm, which reduces the squeeze-film damping which typically occurs in oscillating gaps. The squeeze-film damping associated with electrostatic excitation is also avoided through the use of an integrated electrothermal excitation scheme. Two integrated heating resistors at the center of the resonator structure are excited with a sinusoidal voltage superimposed on a DC voltage. The resulting sinusoidal heating of the bulk silicon near the resistors causes an in-plane deformation of the half-disks due to the bimorph effect.

The deformation of the resonator structure is sensed through a Wheatstone bridge configuration of piezoresistors located at the center of the structure.[15] The piezoresistors that constitute the Wheatstone bridge undergo a differential change in resistance proportional to the mechanical strain occurring at the center of the resonator. The Wheatstone bridge output gives a voltage signal proportional to this strain with minimal offset, hence reducing the complexity of signal readout. The piezoresistors are implemented in the same doping step as the excitation resistors.

To sustain oscillation, the input and output ports of the resonator are connected to an amplifying feedback loop. The Wheatstone bridge output is first amplified and phase-shifted before being rectified and fed back into the excitation elements of the resonator. The initial amplification and phase-shifting are necessary to fulfill the Barkhausen criterion for sustained oscillation. The implementation of this system in this research was with discrete circuit elements arranged on a printed-circuit board. The loop oscillation frequency was read by a frequency counter (Agilent-53131A). A gate time of 1 s was used for all frequency measurements of the system.

FABRICATION

The resonator structures were fabricated using a bulk micromachining technique compatible with standard CMOS fabrication steps. The base substrate for the devices is a 500 μm thick, (100) silicon wafer, 100 mm in diameter. The wafer had a 5 μm ($\pm$1 μm) thick epitaxially grown phosphorus-doped layer on its surface. The wafers were thermally oxidized at 1050 °C to form a 1 μm thick layer of silicon dioxide on the silicon wafer. Subsequently, reactive ion etching (RIE) was used to form diffusion windows in the thermally grown oxide. The exposed silicon areas were doped with boron to achieve a p-type carrier density of approximately 1×10^{19} cm^{-3} to form the Wheatstone bridge and excitation resistor areas. A wet oxidation for 1 h at 1000 °C was then carried out to cover the doped areas with silicon dioxide and simultaneously drive-in the p-type resistors. Contact openings were then etched and aluminum traces were evaporated onto the substrate to connect the resistor areas. Plasma-enhanced chemical vapor deposition (PECVD) was then used to deposit 0.4 μm of silicon nitride and 0.4 μm of silicon dioxide to protect the aluminum traces from long-term atmospheric oxidation.

The PECVD dielectric layers were then etched with RIE to expose the silicon substrate. This step defined the shape of the final resonator structures. Etch windows were created on the down-facing side of the wafer to expose the bulk silicon on the back of the wafer. The wafer was then placed in a KOH bath to etch through the bulk silicon. An electrochemical etch-stop technique was applied to stop the etching at the pn-junction between the n-type epitaxial layer and the p-type substrate. In this way the epitaxial layer determined the thickness of the final resonator structure. After the KOH etching step, a large (1.5 mm × 2 mm) membrane containing the resonator structures remained suspended by the bulk substrate. A final RIE etching of this membrane released the freestanding structures, which were cut into dies using a dicing saw. The final device was measured to be 7 μm thick, owing to variations in the epitaxial layer thickness and the addition of the PECVD layers.

The structures fabricated for this research were subsequently tested for their open and closed loop performance characteristics using the aforementioned in-plane mode. For the 170 μm devices used in this research, Q-factors of 2600 at atmosphere were common, with Q factors at 2 μbar (1.5 mTorr) rising to 6300. This shows anchor loss to be a dominant damping mechanism in these in-plane resonators. Resonance frequencies for the 170 μm devices ranged from 405 to 420 kHz.

To measure the frequency stability of the system, a time domain measurement of the frequency variance known as the Allan variance was used.[21,22] This metric provides a frequency-independent measure of the system frequency stability. The absolute stability can be recovered by multiplying the Allan variance by the system oscillation frequency. Allan variances of 1×10^{-8} were common at atmosphere for the resonators used in this research. These values were found to be highly dependent on the interaction of the resonator with the outside environment: resonators that were not sealed in a measurement chamber had Allan variances that deteriorated up to 1 order of magnitude. The statistical noise added by random molecular motion is greatly reduced in the isolated environment of the measurement chamber. This consideration plays a significant role in packaging these devices for use in the field.

MASS-SENSITIVE BEHAVIOR

The disk resonator structure employed in this research achieves sensitivity to gas analytes through the addition of polymer films to its surface. The volatile analytes used in this research undergo physisoprtion into the polymer films. This leads to a mass increase on the resonator surface, which in turn causes a lowering of the resonant frequency. Larger absorptions of analyte produce larger sensor responses. Hence, it is desirable to choose polymers that have strong physisorption characteristics for the analyte under consideration.

The strength of the thermodynamic force driving the diffusion of the analyte into a given polymer film is characterized by the partition coefficient K. The partition coefficient is an equilibrium constant describing the ratio of the concentration of the analyte in the polymer matrix to its concentration in the surrounding fluid solution, i.e.:

$$K = \frac{c_{poly}}{c_{gas}} \tag{1}$$

where c_{poly} is the concentration of the analyte in the polymer matrix and c_{gas} is the concentration of the analyte in the gas phase. The partition coefficient has an exponential relationship to the inverse of temperature; hence, any heating of the resonator surface has an adverse effect on the chemical sensitivity of the device. A large literature exists with estimates of partition coefficients for different analyte-polymer pairs in both liquid and gas phases.[10,11,23−29]

The chemical sensitivity of the resonator can be described as a change in resonant frequency per unit of analyte concentration. The resonance frequency of the disk resonator structure is determined by the structural stiffness, K_r, and the rotational inertia, J, of the resonator structure. Rotational inertia is used in place of mass because it better describes the in-plane rotational mode of the resonant structure. Therefore, the following equations are generally valid for resonators in a rotational in-plane resonance mode using polymer layers to absorb gas-phase analytes.

The equation describing the resonant frequency is as follows:

$$f_o = \frac{1}{2\pi}\sqrt{\frac{K_r}{J}} \tag{2}$$

Upon analyte sorption, the change in the rotational inertia is the primary contributor to the change in resonant frequency (although changes in elastic modulus of the resonator also occur with sorption, especially in the case of thick sorption films). Stiffness changes due to swelling are considered a second-order effect and are negligible relative to the mass change.[30] Therefore, it is the change in rotational inertia that is of primary consideration in deriving the resonator's chemical sensitivity. The nominal rotational inertia of the layered microstructure can be described by the following equation:

$$J_o = (\rho_{Si} t_{Si} + \rho_{poly} t_{poly}) \int_A r^2 \mathrm{d}A \tag{3}$$

where ρ_{Si} and t_{Si} are the density and thickness, respectively, of the silicon resonator and ρ_{poly} and t_{poly} are the density and thickness, respectively, of the polymer layer. For simplicity, the dielectric layers of the resonator structure are neglected in this analysis. The integral is taken over the lateral geometry of the resonator (this portion of the analysis is omitted for the sake of brevity). The sorption of analyte by the polymer primarily creates a change in polymer density through the dissolution of the analyte molecules into the polymer matrix. The change in polymer density can be denoted by $\Delta\rho_{poly}$. The following equation describes the relative change in mass per unit area on the resonator surface due to mass absorption:

$$\Delta = \frac{\Delta\rho_{poly} t_{poly}}{\rho_{Si} t_{Si} + \rho_{poly} t_{poly}} \tag{4}$$

It follows that the rotational inertia after analyte sorption can be reduced to the following form:

$$J = J_o(1 + \Delta) \tag{5}$$

From the above equation it follows that the new resonant frequency after mass absorption has the following form:

$$f = \frac{1}{2\pi}\sqrt{\frac{K_r}{J}} = \frac{1}{2\pi}\sqrt{\frac{K_r}{J_o(1+\Delta)}} = \frac{1}{2\pi}\sqrt{\frac{K_r}{J}}\sqrt{\frac{1}{1+\Delta}}$$

$$\approx f_o\left(1 - \frac{1}{2}\Delta\right) \tag{6}$$

where the last step is an approximation afforded by a Taylor series expansion. This new resonant frequency is attributable to

an incremental mass change and does not consider changes in the sensor stiffness due to induced stress from, for example, polymer swelling. The relative frequency change due to the change in polymer density is:

$$\frac{\Delta f}{f_o} = -\frac{1}{2}\frac{\Delta\rho_{poly}t_{poly}}{\rho_{Si}t_{Si}+\rho_{poly}t_{poly}} \quad (7)$$

Since the above equation is completely independent of lateral geometric parameters of the resonator or polymer layer, it shows that relative frequency changes due to mass absorption are independent of lateral geometry (assuming the layers of the structure are uniform). Rearranging the above equation to obtain a frequency change per unit of analyte concentration, the chemical sensitivity can be expressed as:

$$S = \frac{\Delta f}{\Delta C} = -\frac{1}{2}\frac{f_o}{\Delta C}\frac{\Delta\rho_{poly}t_{poly}}{\rho_{Si}t_{Si}+\rho_{poly}t_{poly}} = -\frac{1}{2}f_o\frac{\Delta\rho_{poly}}{\Delta C}\frac{t_{poly}}{\rho_{Si}t_{Si}+\rho_{poly}t_{poly}} \quad (8)$$

where ΔC is the change of the analyte concentration. $\Delta\rho_{poly}/\Delta C$ depends solely on the sorption characteristics of the polymer for the analyte of interest and describes the density change of the polymer subject to a given change in analyte concentration. To a first order, S increases linearly with the polymer thickness t_{poly}. The polymer thickness term in the denominator will decrease the sensitivity for thick polymer layers, causing a nonlinearity in the equation.

Assuming a thin polymer film (compared to the silicon thickness), the chemical sensitivity becomes a linear function of the ratio of polymer to silicon thickness. Furthermore, the sorption characteristics of the polymer for a particular analyte and thus the ratio $\Delta\rho_{poly}/\Delta C$ from eq 8 can be written as a function of the partition coefficient K using the ideal gas law, yielding the following simplified equation for S:

$$S = -\frac{1}{2}\frac{f_o}{\rho_{Si}}\frac{KM_aP}{RT}\left(\frac{t_{poly}}{t_{Si}}\right) \quad (9)$$

where K is the analyte-polymer-specific partition coefficient, M_a is the molar mass of the analyte, P is the ambient pressure, R is the ideal gas constant, and T is the absolute temperature. By introducing a factor of 10^6 in the denominator, the chemical sensitivity has units of Hz/ppm.

EXPERIMENTAL SECTION

Polymer Coating. To functionalize the resonator dies with an analyte-absorbing polymer layer, the resonator dies were packaged in a standard 28-pin dual in-line (DIL) package and placed in a spray-coating setup. The spray-coating setup consisted of a commercially available airbrush vertically mounted on a stand. The vertical mounting allowed for the polymer solution to be sprayed directly onto the resonator surface without the polymer subsequently clogging the small gaps of the resonator geometry. The polymer used was (poly)isobutylene (PIB, Sigma-Aldrich) dissolved in a 0.01% w/v solution with toluene. PIB was chosen due to its good film quality and sorption characteristics for VOCs[10,18] For each polymer coating, a reference sample was also coated in order to measure the polymer thickness with a profilometer.

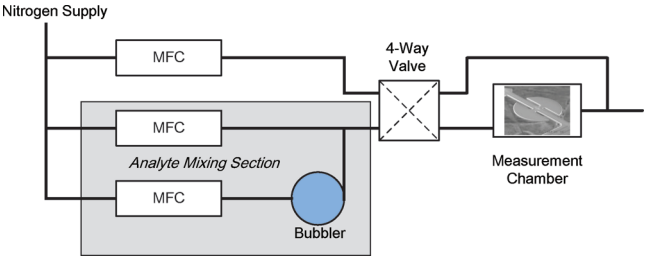

Figure 3. Schematic of the gas manifold system. The flow of the carrier gas is regulated by MFCs, which control the dilution of the analyte vapor.

Analyte Testing. The coated resonators were exposed to controlled analyte concentrations using a custom-made gas manifold system. The gas manifold system consisted of a supply of nitrogen (Airgas, ultra high purity), which was fed to a system of mass-flow controlled gas lines, which connected to a measurement chamber. The nitrogen acted as a carrier gas for analyte dilution. This was accomplished by feeding mass-flow controlled ratios of carrier gas to an analyte-containing bubbler, in which a quartz sand matrix was soaked with the desired analyte. After the bubbler, the analyte reached a temperature-dependent equilibrium concentration in the carrier gas. The bubbler temperature was controlled by a room-temperature water bath, which was kept at 22 °C. The corresponding equilibrium concentration was calculated for a particular analyte by using the Antione coefficients specific to that analyte.[31] This equilibrium concentration was further diluted through the addition of carrier gas after analyte uptake, resulting in the controlled analyte concentration, which was periodically pulsed into the measurement chamber using a four-way valve. When analyte injection was not occurring, a secondary line supplied pure carrier gas to the measurement chamber. The measurement chamber contained the resonator operating in an amplifying feedback loop previously reported.[32,33] A schematic of the gas manifold system is shown in Figure 3.

Analytes used during the experiments included benzene (Sigma-Aldrich, CAS 270709), toluene (VWR, CAS 108883), and *m*-xylene (Sigma-Aldrich, CAS 108383). This trio of analytes is important in environmental monitoring applications and is commonly referred to as BTX. The xylene isomers (*m*-, *o*-, and *p*-xylene) exhibit similar sorption behavior in PIB; hence, *m*-xylene was used as a proxy for all xylene isomers.

RESULTS AND DISCUSSION

Chemical Sensitivity. A disk resonator with an outer radius of 170 μm was coated with several layers of PIB and exposed to linearly increasing concentrations of toluene vapor in the gas phase. The concentrations ranged from 2000 ppm to 16000 ppm of toluene. For each new additional layer of PIB applied, a new test was undertaken. The uncoated resonance frequency of the resonator was 408 kHz, and the thickness of the uncoated resonator was 7 μm including dielectric layers.

Finite element (FEM) simulation results have shown that a temperature elevation of approximately 3 °C/mW occurs on the resonator surface due to the heat dissipation of the excitation resistors and the Wheatstone bridge. The structure was simulated to have a silicon thickness of 6 μm with a 1 μm thick dielectric layer. Each excitation resistor and Wheatstone bridge resistor has a resistance of 500−600 Ω. For the voltages applied during

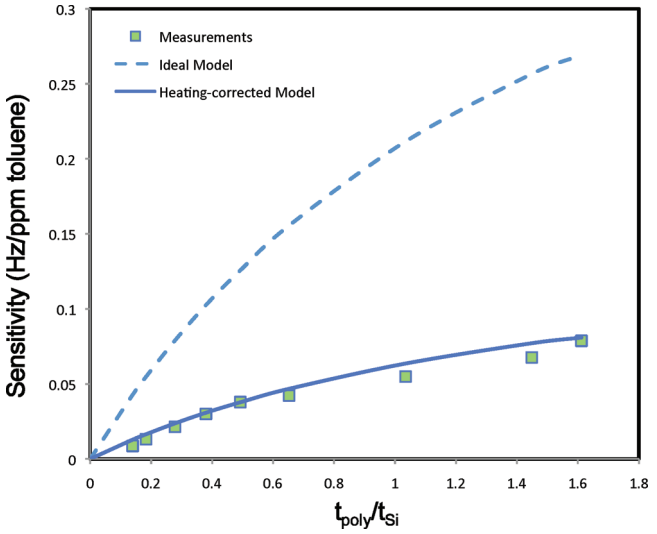

Figure 4. The chemical sensitivity to toluene as a function of normalized polymer thickness, where the dashed line is the ideal sensitivity predicted from eq 8, the solid line is the sensitivity predicted by eq 8 with the heat-adjusted partition coefficient, and the squares are the experimentally measured sensitivities.

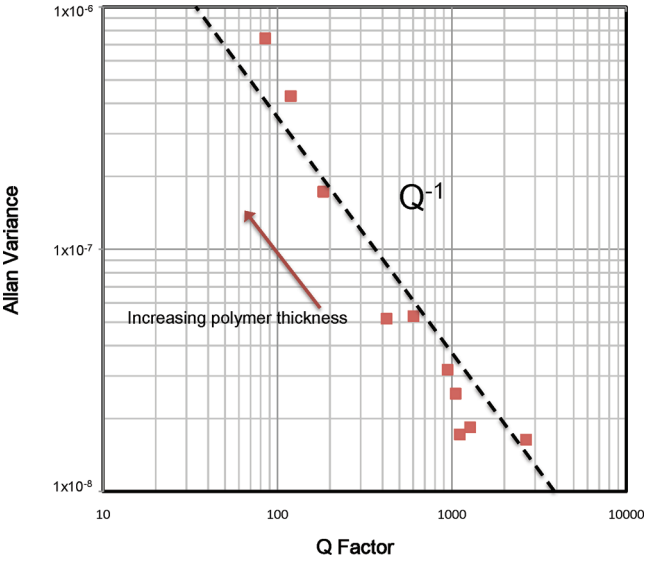

Figure 5. Allan variance as a function of *Q*-factor for a resonator with different polymer film thicknesses.

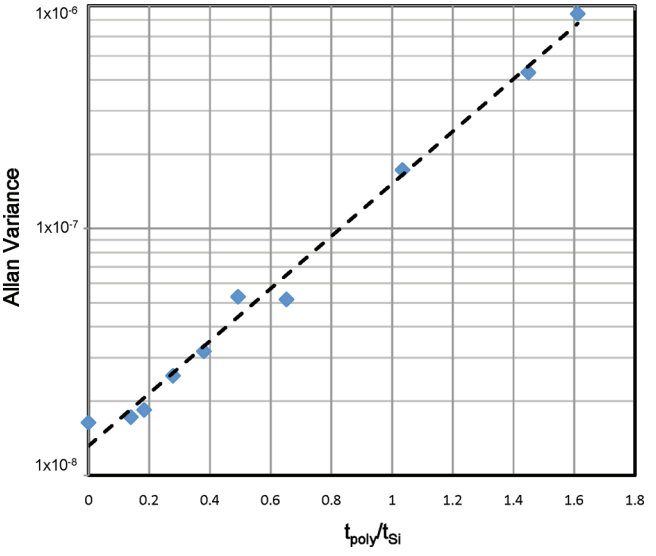

Figure 6. Allan variance of a disk resonator as a function of normalized polymer film thickness.

device testing, the Wheatstone bridge produces roughly 8 mW of heating power and the combined heating power of the excitation resistors is 3.8 mW, causing a temperature elevation of roughly 35 °C on the resonator surface. This temperature elevation reduces the absorptive effects of the polymer applied to the resonator surface for the purpose of mass-sensing.

Assuming a 35 °C temperature elevation, the toluene−PIB partition coefficient is lowered from published values of 1030[10] down to 300. This heating-corrected partition coefficient is obtained by curve-fitting to previously published partition coefficient data. The temperature dependence of K for the polymer used in this research can be used to extrapolate a new heating corrected partition coefficient based on the published slope of ln K vs $1/T$ curves.[24] Figure 4 shows the heating-corrected chemical sensitivity and the experimentally measured chemical sensitivity vs. the normalized polymer thickness, and they are found to be in good agreement. Given the large range of polymer thicknesses investigated, the full nonlinear sensitivity model of eq 8 was used for both the ideal and heating-corrected models of Figure 4.

With each subsequent layer of PIB, the resonant frequency of the resonator decreased, in accordance with eq 2 and eq 3. The chemical sensitivity increased, but was found to be below the trend expected from eq 8 (shown as the dashed line in Figure 4). The cause of this relative decrease in sensitivity is the heating of the polymer layer by the excitation and sensing resistors used in the resonator structure.

Limit of Detection. The limit of detection (LOD) for a particular analyte is defined as 3 times the ratio of the oscillator system's frequency noise to its analyte-specific sensitivity:

$$\mathrm{LOD} = 3\frac{\mathrm{Var}(f)}{S} = 3\frac{f_o \mathrm{Var}_{\mathrm{Allan}}(f)}{S} \qquad (10)$$

where $\mathrm{Var}(f)$ is used to refer to the absolute frequency variance of the system oscillation frequency, $\mathrm{Var}_{\mathrm{Allan}}(f)$ is the Allan variance, and a prefactor of 3 is used in order to distinguish frequency changes due to mass-change from the noise level. The LOD metric is the ultimate measure of performance for a chemical sensor system.

The LOD is shown to be highly dependent on the thickness of the polymer layer on the resonator surface. The viscoelastic properties of the polymer result in the dissipation of mechanical energy from the bulk silicon of the resonator. This results in a reduction of the resonator *Q*-factor with increasing polymer thickness. Measurements of the *Q*-factor taken after each incremental polymer coating are used to find the effect of polymer thickness on *Q*-factor. The change in *Q*-factor in turn affects a change in the Allan variance and a $1/Q$ relationship was found, similar to what has been previously reported[13] and is shown in the log−log plot of Figure 5 by a regression of Allan variance on *Q*. The relationship of Allan variance to normalized polymer thickness is shown to be exponential in nature. This relationship is plotted in the log−linear plot of Figure 6. The exponential

dx.doi.org/10.1021/ac1029902 |*Anal. Chem.* 2011, 83, 3305–3311

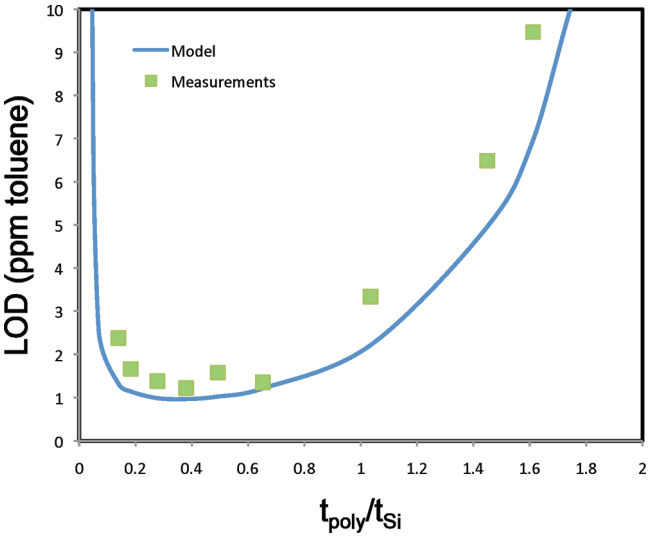

Figure 7. Model of LOD for toluene (solid line) and measured LODs for toluene (squares) as a function of normalized polymer thickness. Minimum limit of detection was 1.2 ppm.

relationship between polymer thickness and Allan variance implies an inverse exponential relationship between polymer thickness and *Q*-factor.

From the exponential dependence of frequency variance on polymer thickness shown in Figure 6, the definition of LOD shown in eq 10 becomes a ratio of an exponential function of polymer thickness to a linear function of polymer thickness (using the first-order sensitivity approximation of eq 9). Therefore, the polymer will have an optimal thickness that minimizes LOD. The Allan variance of the resonator can be described by the following equation:

$$\mathrm{Var}_{\mathrm{Allan}}\left(\frac{t_{\mathrm{poly}}}{t_{\mathrm{Si}}}\right) = \mathrm{Var}_{\mathrm{o}} e^{\alpha\left(\frac{t_{\mathrm{poly}}}{t_{\mathrm{Si}}}\right)} \qquad (11)$$

where $\mathrm{Var}_{\mathrm{o}}$ is the initial Allan variance of the uncoated resonator and α is a fitting factor derived from empirical observations by regressing the measured Allan variance against the normalized polymer thickness. The fitting factor α has values ranging from 2 to 11 for the resonators in this research and is proportional to the resonator silicon thickness t_{Si}. Combining eq 9, eq 10, and eq 11 produces an analytical model which closely matches the experimentally measured LODs for toluene and agrees with the shape of LOD curves derived in previous theoretical work.[34] Figure 7 compares this model with the experimental results. In Figure 7, the model has been adjusted to account for polymer heating as in Figure 4.

For toluene, the minimum limit of detection was 1.2 ppm. Approximately 2.6 μm of PIB achieved this limit on a 7 μm thick resonator, corresponding to a normalized polymer thickness of 0.37.

Calibration Curves. A series of calibration curves were measured for the VOCs benzene, toluene, and *m*-xylene. These calibration curves were measured with a PIB thickness of 4.5 μm, corresponding to a normalized thickness of 0.625. From the data shown in Figure 7, this polymer thickness is still within the region of minimum LOD for toluene. Because of the strong exponential relationship of frequency stability on polymer thickness, this same optimal region of detection can be expected when applied

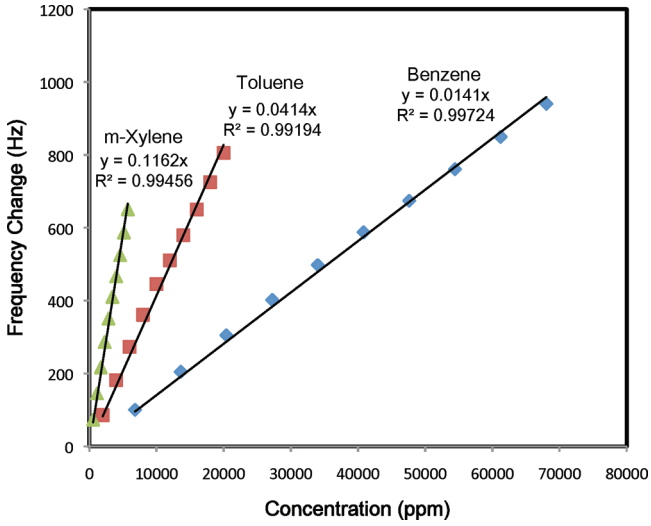

Figure 8. Gas-phase calibration curves for benzene (diamonds), toluene (squares), and *m*-xylene (triangles).

Table 1. LODs and Partition Coefficients for Benzene, Toluene, and *m*-Xylene

analyte	measured LOD, ppm	predicted LOD, ppm	published *K*	heat-adjusted *K*
benzene	5.3	4.0	360[10]	108
toluene	1.2	1.0	1030[10]	300
m-xylene	0.6	0.5	2137[25]	642

to other analytes. Equation 10 can be modified to correct for the use of different analytes, as only the sensitivity term need be changed through the use the different analyte-specific partition coefficients. Figure 8 shows the calibration curves for benzene, toluene, and *m*-xylene.

If one accounts for the polymer heating, the calibration curves agree well with published data for the PIB partition coefficients for benzene, toluene, and *m*-xylene. In particular, the ratios of the chemical sensitivities for *m*-xylene, toluene, and benzene of 0.116, 0.0414, and 0.0141 Hz/ppm agree with ratios of published partition coefficients for PIB of *m*-xylene, toluene, and benzene, respectively. Assuming a PIB−toluene gas-phase partition coefficient of 1030,[10] this analysis yields a PIB−*m*-xylene partition coefficient of 2560, and a PIB−benzene partition coefficient of 334. These values agree well with published data (see Table 1).

Additionally, the model of eqs 9, 10 and 11 predicts LOD values close to the measured LODs of the three analytes. These data, along with published and heat-adjusted partition coefficients for each analyte, are summarized in Table 1.

From the data presented in Table 1, it becomes clear that the heat dissipation caused by the integrated resistive elements causes a significant decrease in the sensitivity of the coated resonator structure, thus affecting the LOD. The results of Figure 4 indicate that LOD could be reduced by 3−5 times by reducing the heating power. The heating power can be reduced by using lower excitation voltages. However, this approach increases the frequency noise, resulting in higher LODs. Sensors could alternatively be designed to reduce heating without affecting Allan variance, which would hence yield improvements in LOD.

dx.doi.org/10.1021/ac1029902 |*Anal. Chem.* 2011, 83, 3305–3311

SUMMARY

In summary, a chemical sensor based on polymer-coated in-plane resonators has been presented. The in-plane mode of the resonator structure allows it to achieve high *Q*-factors, allowing for reduced frequency variance in viscous environments. The resonator uses a silicon-based CMOS-compatible fabrication process, allowing the integration with CMOS electronics to implement a self-contained sensor system.

Characteristics of the analyte response of the sensor were measured and used to build a model for the sensitivity and LOD. Measurements were carried out on 7 μm thick resonators with a 170 μm outer radius. The functionalizing polymer was PIB, and the analytes tested were gaseous benzene, toluene, and *m*-xylene. The derived models were found to be in agreement with the measured results. Chemical sensitivity to first-order has a linear dependence on polymer thickness whereas frequency variance was found to have an exponential dependence on polymer thickness. This leads to an optimal region of polymer thickness for which the LOD is minimized. The exact nature of the exponential dependence of frequency variance is subject to a fitting parameter which is dependent on device thickness.

Limits of detection for benzene, toluene, and *m*-xylene were found to be 5.3 ppm, 1.2 ppm, and 0.6 ppm, respectively. These LODs were found to be close to those predicted by the derived model, and the low to sub-ppm LODs achieved are close to those shown through research on cantilever-based detection of VOCs.[18] If the polymer layer is not heated, LOD reduction by a factor of 5 can be achieved. Given this heating optimization, the high-Q gravimetric sensing platform used in this research should be able to accomplish LODs in the mid-ppb range for VOCs.

This work has shown the various advantages of the sensor system in the detection of VOCs in a gaseous environment. With further optimization, these sensors have the possibility of co-integration with CMOS readout circuitry, thus presenting a distinct advantage over SAW-based sensors. With localized functionalization of selective polymers, these sensors also have the possibility of being integrated into sensor arrays. Such sensor arrays have the possibility of analyzing analyte mixtures to yield a versatile self-contained VOC detection system.

AUTHOR INFORMATION

Corresponding Author

*E-mail: gt0914a@mail.gatech.edu.

ACKNOWLEDGMENT

This work was funded in part by the National Science Foundation through awards ECCS-0601467 and ECCS-0824017. The authors thank the NRC Cleanroom staff at the Georgia Institute of Technology. The authors also thank the BEL Laboratory at the ETH Zurich for their contribution of knowledge and technical support. Finally the authors would also like to thank Sensirion for providing the mass flow controllers used in the gas manifold system.

REFERENCES

(1) King, W. H. *Anal. Chem.* **1964**, *36*, 1735–1739.
(2) Yang, Y. T.; Callegari, C.; Feng, X. L.; Ekinci, K. L.; Roukes, M. L. *Nano Lett.* **2006**, *6*, 583–586.
(3) Li, P.; Li, X.; Zuo, G.; Liu, J.; Wang, Y.; Liu, M.; Jin, D. *Appl. Phys. Lett.* **2006**, *89*, 074104.
(4) Li, P.; Li, X. *J. Micromech. Microeng.* **2006**, 2539.
(5) Boisen, A.; Thaysen, J.; Jensenius, H.; Hansen, O. *Ultramicroscopy* **2000**, *82*, 11−16.
(6) Fritz, J.; Baller, M. K.; Lang, H. P.; Rothuizen, H.; Vettiger, P.; Meyer, E.; Güntherodt, H. -J.; Gerber, C.; Gimzewski, J. K. *Science* **2000**, *288*, 316–318.
(7) Patel, R.; Zhou, R.; Zinszer, K.; Josse, F.; Cernosek, R. *Anal. Chem.* **2000**, *72*, 4888–4898.
(8) Li, Z.; Jones, Y.; Hossenlopp, J.; Cernosek, R.; Josse, F. *Anal. Chem.* **2005**, *77*, 4595–4603.
(9) Lu, C.-J.; Zellers, E. T. *Anal. Chem.* **2001**, *73*, 3449−3457.
(10) Hierlemann, A.; Ricco, A. J.; Bodenhöfer, K.; Göpel, W. *Anal. Chem.* **1999**, *71*, 3022–3035.
(11) Hierlemann, A.; Zellers, E. T.; Ricco, A. J. *Anal. Chem.* **2001**, *73*, 3458–3466.
(12) Cleland, A. N.; Roukes, M. L. *J. Appl. Phys.* **2002**, *92*, 2758–2769.
(13) Albrecht, T. R.; Grutter, P.; Horne, D.; Rugar, D. *J. Appl. Phys.* **1991**, *69*, 668–673.
(14) Martin, S. J.; Ricco, A. J.; Niemczyk, T. M.; Frye, G. C. *Sens. Actuators* **1989**, *20*, 253−268.
(15) Jae Hyeong, S.; Brand, O. *J. Microelectromech. Syst.* **2008**, *17*, 483–493.
(16) Voiculescu, I.; Zaghloul, M. E.; McGill, R. A.; Houser, E. J.; Fedder, G. K. *IEEE Sens. J.* **2005**, *5*, 641–647.
(17) Bargatin, I.; Kozinsky, I.; Roukes, M. L. *Appl. Phys. Lett.* **2007**, *90*, 093116.
(18) Lange, D.; Hagleitner, C.; Hierlemann, A.; Brand, O.; Baltes, H. *Anal. Chem.* **2002**, *74*, 3084–3095.
(19) Vancura, C.; Li, Y.; Lichtenberg, J.; Kirstein, K.-U.; Hierlemann, A.; Josse, F. *Anal. Chem.* **2007**, *79*, 1646–1654.
(20) Naeli, K.; Brand, O. *J. Appl. Phys.* **2009**, *105*, 014908.
(21) Allan, D. W. *Proc. IEEE* **1966**, *54*, 221–230.
(22) Allan, D.; Hellwig, H.; Kartaschoff, P.; Vanier, J.; Vig, J.; Winkler, G. M. R.; Yannoni, N. F. *Proc. Annu. Symp. Freq. Control* **1988**, 419–425 .
(23) Grate, J. W.; Kaganove, S. N.; Bhethanabotla, V. R. *Anal. Chem.* **1998**, *70*, 199–203.
(24) Hierlemann, A.; Ricco, A. J.; Bodenhöfer, K.; Dominik, A.; Göpel, W. *Anal. Chem.* **2000**, *72*, 3696−3708.
(25) Jones, Y. K.; Zhonghui, L.; Johnson, M. M.; Josse, F.; Hossenlopp, J. M. *IEEE Sens. J.* **2005**, *5*, 1175–1184.
(26) Martos, P. A.; Saraullo, A.; Pawliszyn, J. *Anal. Chem.* **1997**, *69*, 402–408.
(27) Saraullo, A.; Martos, P. A.; Pawliszyn, J. *Anal. Chem.* **1997**, *69*, 1992–1998.
(28) Patrash, S. J.; Zellers, E. T. *Anal. Chem.* **1993**, *65*, 2055–2066.
(29) Schierbaum, K. D.; Göpel, W. *Synth. Met.* **1993**, *61*, 37−45.
(30) Wenzel, M. J.; Josse, F.; Heinrich, S. M.; Yaz, E.; Datskos, P. G. *J. Appl. Phys.* **2008**, *103*, 064913.
(31) Weissberger, A. *Organic Solvents*; 4th ed.; Wiley: New York, 1986; Vol. II.
(32) Demirci, K. S.; Seo, J. H.; Truax, S.; Beardslee, L. A.; Luzinova, Y.; Mizaikoff, B.; Brand, O. *Proc. IEEE Micro Electro Mech. Syst., 22nd, 2009* **2009**, 284–287.
(33) Truax, S.; Demirci, K. S.; Hierlemann, A.; Brand, O. *Transducers 2009, Int. Conf. Solid-State Sens., Actuators Microsyst., Dig. Tech. Pap., 15th, 2009* **2009**, 1838–1841 .
(34) Dufour, I.; Lochon, F.; Heinrich, S. M.; Josse, F.; Rebiere, D. *IEEE Sens. J.* **2007**, *7*, 230–236.